Experimental Report

14/01/2014

Proposal:	**9-10-1299**	**Council:**	10/2012	
Title:	Spatio-temporal instabilities in viscoelastic surfactant solutions			
This proposal is a new proposal				
Research Area:	Soft condensed matter			

Main proposer: **MUETZE Annekathrin**

Experimental Team: LUTZ BUENO Viviane
MUETZE Annekathrin
HEUNEMANN Peggy

Local Contact: SCHWEINS Ralf
PORCAR Lionel

Samples: Cetylpyridinium chloride/ $C_{21}H_{38}ClN$
Sodium salycilate/ $C_7H_5NaO_3$
Lithium salycilate/ $HOC_6H_4CO_2Li$

Instrument	Req. Days	All. Days	From	To
D22	0	3	10/05/2013	13/05/2013

Abstract:

We want to investigate the flow dynamics of two comparable wormlike micellar surfactant solutions that show special shear-induced features. Previous small-angle light and neutron scattering experiments on such systems showed that the most valuable structural information are given in the U-SANS-regime, from which we stayed out of range so far. Rheo-SANS experiments on D11, with lowest momentum transfer and lowest background possible should fill this gap and help elucidating the meso- and small-length scales, where these unique sample-properties are caused. For the foreseen time-triggered rheo-SANS experiment a rheometer with couette-setup and an inhouse development for the technical linkage (rheometer- and SANS-instrument) will be provided by ETH.

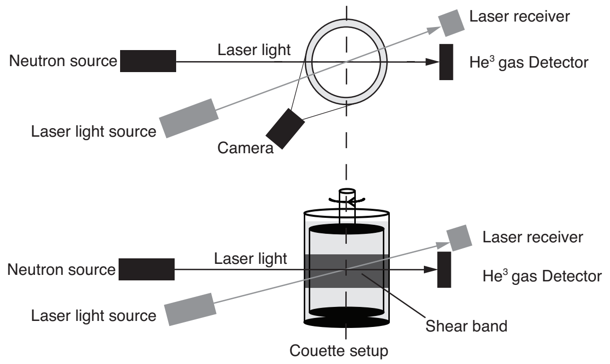

Figure 1: Scheme of the experimental setup to determine the rheological behaviour, the laser light transmittance, the small angle neutron scattering, and to visualise the shear band formation.

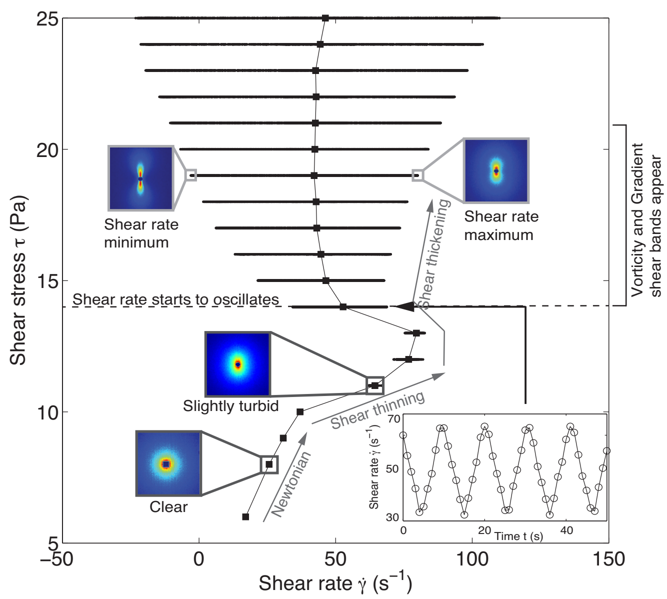

Figure 2: Shear stress versus shear rate for 40 mM CPCl/NaSal solution (24 °C, 100% D_2O). Each data point of the shear rate oscillation is given in the diagram and is shown by horizontal lines. The figure in the lower right shows a cutout of the oscillation of the shear rate as function of time at $\tau = 14$ Pa. For the Newtonian regime, shear thinning regime, and the shear thickening regime small angle scattering pattern are shown (detector distance 6 m, wave length 6 Å).

In this proposal 9–10–1299, we investigated the alternating appearance of turbid and clear vorticity and gradient shear bands formed by elongated wormlike micelle surfactant solutions to obtain insights into the formation of gradient and vorticity shear bands that appear simultaneously. For this purpose we used a viscoelastic surfactant solutions based on an equimolar mixture of cationic cetylpyridinium chloride CPCl and either the monovalent salts: lithium, sodium, or potassium salicylate (LiSal, NaSal, KSal) and the bivalent salts calcium salicylate ($CaSal_2$), by using a time-triggered rheo-SANS setup at the SANS-instrument D22

The data supplied by the SANS (momentum transfer q, scattering intensity I) and rheometer-measurements (shear stress, shear rate), as well as the ones coming from the laser light signal (sample transmittance) will be recorded simultaneously (see setup in Fig. 1). A circular aperture of 12 mm in diameter was used to shorten the experimental time. The data is acquired at wavelength $\lambda = 6\,\text{Å}^{-1}$ ($\lambda = 11\,\text{Å}^{-1}$), sample-to-detector distance SD of 2.8 , 5.6 and 17.6 m (17.6 m) and collimation of 2.8 , 5.6 and 17.6 m (17.6 m, respectively), to cover a total q-range of 10^{-3} to $10^{-0.6}\,\text{Å}^{-1}$. In our time-triggered SANS experiments, all neutron events are summed at the shear rate minimum/maximum to one scattering pattern each (Fig. 2).

The rheological behaviour of the exemplary salt-surfactant solution NaSal/CPCl at 24 °C is shown in Fig. 2, using a rheometer Couette cell setup in rotational mode. To simplify the resulting curves we mark the mean values of the shear rate for each shear stress with a big symbol and connect them (see Fig. 2).

Furthermore, shows Fig. 3 a detailed insight into the oscillation of the shear rate (a), the respective laser-light transmission measurements (c), and the simplified visual images (b) of the gradient and vorticity shear bands over time. Notice, the laser-light is positioned perpendicular to the Couette axis and has the same level like the neutron beam.

For low shear stresses ($\tau \leq 9$ Pa) the solution stays clear and shows a Newtonian flow behaviour (Fig. 2), where the micelles are arranged in an isotropic (chaotic) way (see 2D-scattering pattern from small angle neutron scattering named clear in the Newtonian regime in Fig. 2). With increasing shear stress ($\tau < 12$ Pa) the viscosity changes to a shear thinning behaviour. The solution gets

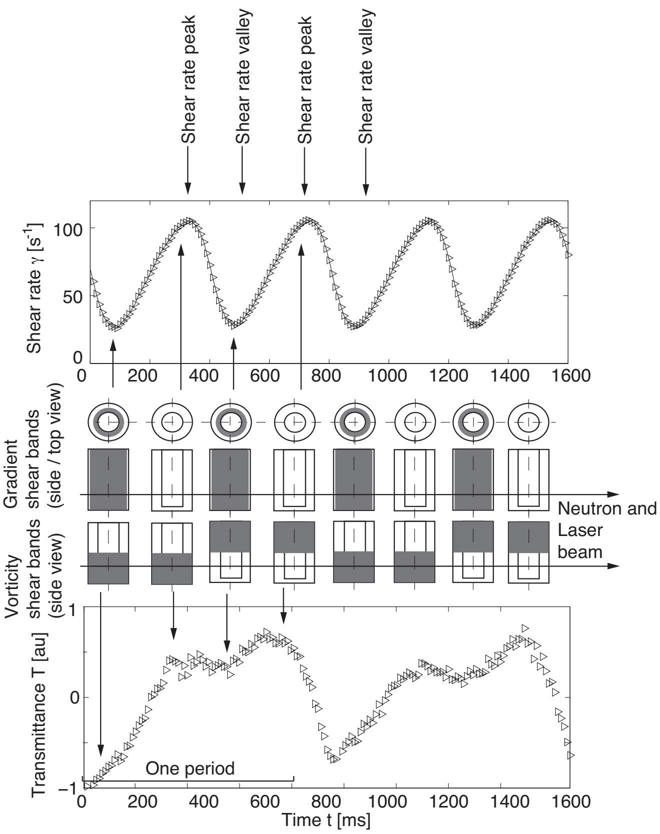

Figure 3: (a) Shear rate $\dot{\gamma}$, (b) simplified optical images (top and side view of the Couette cell) and (c) laser light transmittance T versus time t; the horizontal arrow in (b) indicates the laser-light and neuton beam (40 mM CPCl/LiSal, 100 % D_2O, 25 °C, 20 Pa).

slightly turbid and streaks appear, because the micelles start to align (see 2D-scattering pattern named slightly turbid in the shear thinning regime in Fig. 2). Above a critical shear stress value ($\tau \approx$ 14 Pa) the solution gets shear thickening. Additionally, the shear rate starts to oscillate and vorticity and gradient shear bands appear, due to a further alignment of the micelles [1]. We distinguish vorticity (horizontal) and/or gradient (vertical) shear bands. The vorticity shear bands form strips along the flow direction which are located perpendicular to the Couette cell axis [2, 3]. In contrast, gradient bands form concentric alternating layers around the Couette axis (see Fig. 3 (b)) [3]. Both kinds of shear bands appear simultaneously, in which the vorticity shear bands dominated the visual effect (gradient shear bands are not visible by eye) and the gradient shear bands the rheological response, i.e. the shear rate frequency ($2.5 \cdot 10^{-3}\,\mathrm{s}^{-1}$) is the same like the phase change (turbid, clear) of the gradient shear bands ($2.5 \cdot 10^{-3}\,\mathrm{s}^{-1}$). Contrary to this alternate the phases of the vorticity shear bands ($1.24 \cdot 10^{-3}\,\mathrm{s}^{-1}$) with half the frequency of the shear rate (see Fig. 3 (b) and (c)). We conjecture that the shear rate oscillation is caused by a drastic change in the micelle arrangement from isotropic (chaotic) in the clear phase to anisotropic (alignment) in the turbid phase. The contradiction of the scattering pattern to this assumption is due to the following explanation: The vorticity shear band (only one band is detected) changes from turbid to clear with half the frequency of the shear rate, therefore the detected neuron events of the turbid and clear phase is the same for the shear rate maximum and minimum (see the bottom row of Fig. 3 (b)). From this it follows that the main influencing parameter has to be the gradient shear bands [1]. At the shear rate minimum the scattering pattern shows a typical butterfly pattern (Fig. 2), which indicates highly aligned micelles (turbid phase) at the shear rate minimum. Conversely, the sum of all neutron events at the shear rate maximum shows a slightly anisotropic scattering pattern (Fig. 2), which indicated a mixture of aligned (turbid) and chaotic (clear phase) arranged micelles, where the chaotically arranged micelles are predominant. This indicates a mainly clear phase from the gradient shear bands at the shear rate maximum and only a slight influence of turbid phases from the vorticity shear bands.

To summarize, the differences in the SANS pattern mainly results from the gradient shear bands. In particular, at the shear rate minimum (butterfly pattern) a higher number of turbid shear bands were detected (micelles are aligned), compared to the slightly anisotropic pattern at the shear rate maximum, which indicates a higher number of detected clear bands. This supports our hypothesis, that the shear rate is dominated by gradient shear bands and vorticity and gradient shear bands appear simultaneously.

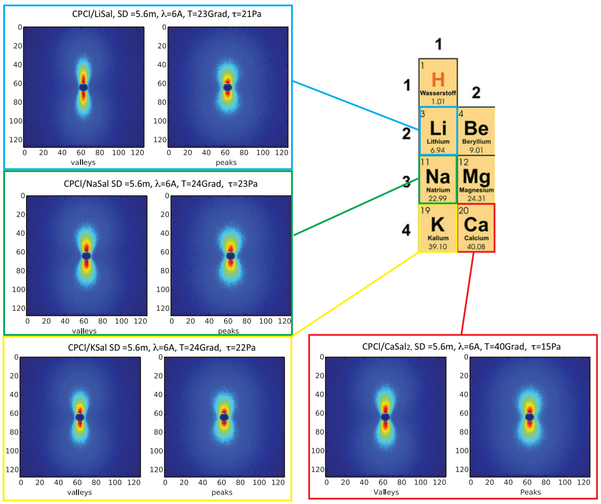

Figure 4: The scattering pattern at the shear rate minimum (valley) and shear rate maximum (peak) are given for the four analysed solutions (CPCl with LiSal, NaSal, KSal, or $CaSal_2$) The sample-detector distance, the wavelength, temperature and shear stress are given in each figure caption (100 % D_2O). On the top right hand a cutout of the table of elements for the used counterions (salts) are shown.

The appearance and the number of gradient shear bands according to the used counterion was investigated further to the salt-surfactant systems, LiSal/CPCl, NaSal/CPCl, KSal/CPCl, and $CaSal_2$/CPCl. For all solutions the temperature and shear stress was adapted in such a way that two vorticity shear bands appear. In doing so, the transmittance measurements shows that LiSal show one gradient shear band, NaSal two and KSal ($CaSal_2$/CPCl three gradient shear bands simultaneously with the vorticity shear bands [1]. An increasing in the number of shear bands causes to an overlapping of detected clear and turbid phases, i.e. the detected time-resolved scattering pattern are more smeared.

In summary, we show simultaneous appearance of vorticity and gradient shear bands using the detected laser signal, shear rate, video visualisation and SANS measurements. We could show that with increasing molecular mass (monovalent salts) the number of gradient shear bands decrease for the same experimental conditions (number of vorticity shear bands, temperature und shear stress). In the two-vorticity shear band state the counterion valency has no influence on the number of gradient shear bands.

From the data acquired from these triggered rheo-SANS experiments in the shear band regime, so far only common structural properties of both shear band types were accessible, but the data analysis for these experiments are not finished until now.

References

[1] A. Mütze, P. Heunemann, E. J. Windhab, and P. Fischer. *J. Rheol.*, (submitted), 2013.

[2] V. Herle, P. Fischer, and E.J. Windhab. *Langmuir*, 21:9051–9057, 2005.

[3] P.D. Olmsted. *Rheol. Acta*, 47:283–300, 2008.